Article

ADSORPTION PROCESS OF PESTICIDE ON SWCNT FUNCTIONALIZED AND CROSSLINKED WITH CHITOSAN USING PM3 SEMI-EMPIRICAL METHOD AND MONTE CARLO SIMULATION

Alfredo de Jesús-González[a] and Norma Aurea Rangel-Vázquez[a,*]

[a]Departamento de Posgrado e Investigación, Instituto Tecnológico de Aguascalientes, PO Box 20256 Aguascalientes, México

Received: 02/23/2024; accepted: 04/08/2024; published online: 06/25/2024

In this work, using the PM3 semi-empirical method, the oxidation of the single-walled carbon nanotube (SWCNT) was studied by sulfuric and nitric acid for the incorporation of carbonyl (C=O), phenol (OH) and carboxylic (COOH) groups in the C=C bonds present on the surface of the nanotube. Subsequently, the crosslinking of the oxidized SWCNT (SWCNTox) and chitosan (Q) was observed through hydrogen bonds of the C=O and OH bonds with 2.34 Å, the process was endothermic and soluble in polar solvents due to the presence of OH and NH groups in the structure of SWCNTox/Q. The Monte Carlo modeling allowed to study the adsorption of pesticides in the SWCNTox/Q at different temperatures, where the QSAR (quantitative structure activity relationship) properties allowed predicting the behavior of the pesticides, that is, the degree of hydrophobicity (log P) and accessible surface area (ASA) were important parameters in the evaluation of SWCNTox/Q as an adsorbent and surface interacting with pesticides respectively. Finally, the adsorption was a physisorption process due to the electronegativity of the CO, OH, NH_2, NH and C=O bonds.

Keywords: pesticides; adsorption; simulation.

INTRODUCTION

Water represents the most important characteristic for the environment, however, due to rapid population, economic and industrial growth, pollution problems produce different diseases in the short, medium, and long term. There are various organic pollutants such as, pesticides, domestic and industrial waste, which cause various health problems as cancer, hormonal and nervous system disorders, among others.[1,2]

Pesticides represent 24 thousand million dollars in market value and an increase of 10 billion was determined for the year 2022.[3,4] Pesticides are used as a protection barrier for crops against a diversity of pests, disease control and food preservation, however, they produce various diseases in human health and the environment.[5] Contamination occurs in the agricultural industry because the degradation products are present in groundwater and surface water, but the activity of the pesticide is affected by the characteristics of the soil, as well as the type of application, management, and properties of the pesticide.[6-8]

Glyphosate, atrazine and diuron represent the main pesticides due to their resistance to degradation and the ability to magnify themselves in the food chain.[9] Glyphosate is a non-volatile compound, stable to sunlight and soluble in water. It decreases the production of aromatic amino acids necessary for protein synthesis because the activity of the plant enzyme 5-enolpyruvyl-shikimate-3-phosphate synthase (EPSPS) present in fungi and plants decreases.

Glyphosate degradation generates AMPA (amino methyl phosphonic acid), sarcosine, glycine. AMPA has a shelf life between 76 and 240 days while glyphosate of 91 days.[5,10] On the other hand, diuron is a phenyl urea pesticide. According to the European Commission, it is considered a priority pesticide due to environmental pollution and increases the incidence of poisoning of fish and other aquatic species, due to runoff and residential pesticide, besides is used to control weeds, grasses, and shrubs, however, it stops photosynthesis.[8,11] Atrazine belongs to the group of organochlorines triazine pesticides. It acts with the D1 protein of photosystem II present in plant cells (PSII), modifying the electron transport chain, that is, bromoacyl also acts on PSII, while paraquat acts on photosystem I (PSI).

Therefore, the pesticide is the only electron acceptor, redirecting the electrons that go to photosystem I (PSI), thus this reaction produces the formation of superoxide radicals. Atrazine is highly soluble in water and is absorbed by the roots or leaves of grasses and is used before or after weeds germinate. Atrazine produces irritation and damage to different organs and sterility.[12]

On the other hand, adsorption is an economic technique, easy to operate, efficient, eliminates the presence of contaminant residues and allows the use of different adsorbents, which have the capacity for regeneration and reuse. The main adsorbents are carbon nanotubes (CNT), chitosan biopolymer membrane, graphene oxide, activated carbon, zeolites and polymeric materials functionalized with amine groups.[13] Carbon nanotubes (CNTs) are allotropes of carbon with a hexagonal structure, formed from a sheet of graphene, which is rolled into cylinders. CNTs are classified as single-walled (SWCNT) and multi-walled (MWCNT). SWCNTs have a diameter of 1 nm with a length to diameter ratio of 1000.[14,15]

SWCNTs have been used in the adsorption of triazines, sulfonylureas, organophosphorus, organochlorine, and multiclass pesticides,[16] heavy metals,[17] phenols[18] and dyes.[19] But is necessary to improve its properties by increasing its selectivity and adsorption capacity due to adding functional groups.[13] SWCNT functionalization uses OH, C=O and NH groups through chemical oxidation or polymer coatings,[20-23] for increasing the dispersion in water and the contact surface area, which increase the adsorption capacity of different contaminants.[24-26] Chitosan (Q) is a polysaccharide derived from the deacetylation of chitin, biocompatible and biodegradable and widely used in water treatment, membranes, biomedicine, sensors, among others. It is used as fillers for SWCNT or SWCNT/nanoparticle compounds for increasing the mechanical and chemical properties due to covalent bonds at the interface of these new materials.[18,27]

Finally, computational chemistry represents an effective tool, which is used in various areas of research for the development of new compounds and, recently, in adsorption processes;[28-30] where the computational chemistry allows predicting energetic properties and QSAR (quantitative structure activity relationship) from

*e-mail: norma.rv@aguascalientes.tecnm.mx

computational methods with principles based on molecular and quantum mechanics.[31]

QSAR properties are those that depend on molecular structure and behavior in biological activities; among these properties are the molecular mass (m), volume (V), molecular surface area (AS), octanol-water partition coefficient (log P) and the accessible surface area (ASA) that are related to the geometry and optimization.[32] The ASA is the surface area of an adsorbent that can interact with a solvent and is calculated from the radius of a water molecule (1.4 Å).[33] However, considering that, in the adsorption process the adsorbent is in contact with the contaminant, it is important to carry out these studies.

Thus, the objective of this research was to determine the energetic properties and QSAR, as well as the electronic distribution of the adsorption of various pesticides (glyphosate, diuron and atrazine) using SWCNT functionalized (SWCNTox) and crosslinked with chitosan (Q) (SWCNTox/Q) at 291.15 and 298.15 K, respectively.

EXPERIMENTAL

The PM3 semi-empirical method of the Hyperchem 8v software was used to determine the optimization or energy minimization geometry based on the positions in space of each pesticide, the SWCNT functionalized (SWCNTox) and the crosslinked SWCNTox/Q, selecting the Polak-Ribiere algorithm, which uses the conjugate gradient method with a convergence level of 0.001 kcal mol^{-1} $Å^{-1}$ and 5000 iterations, respectively. The Monte Carlo simulation determined the behavior of the molecules at different temperatures (291.15 and 298.15 K). QSAR and energetic properties such as Gibbs free energy (G), enthalpy (H), entropy (S), dipole moment and the MESP (map of electrostatic potential) of each SWCNTox/Q-pesticide adsorption were obtained at 20 runs steps in empty mode.

Properties of individual molecules

The SWCNT (see Figure 1a) was functionalized with hydrogen atoms by default, corresponds to a zig-zag (5.0) structure, a length of 11.2967 Å and a diameter of 3.9620 Å, log P of 11.71, mass of 730.74 amu, AS of 571.61 $Å^2$, volume (V) of 459.48 $Å^3$ and radius (r) of 5.1484 Å. Chitosan (see Figure 1b) corresponded to 80% deacetylation, where the QSAR properties indicated a log P of –8.71, mass of 865.84 amu, AS of 834.61 $Å^2$, volume of 708.79 $Å^3$ and a radius of 5.5311 Å, respectively.

Table 1 shows the thermodynamic and QSAR properties of the individual pesticides obtained by the PM3 semi-empirical method. Gibbs free energy and heat of formation indicated that glyphosate[34-36] and diuron[37-40] are exothermic and spontaneous while atrazine[40,41] is spontaneous and endothermic. The dipole moment of glyphosate was attributed to the electronegativity of oxygen, as well as the presence of the phosphonate and carboxylic acid groups (see Figure 2a), while the log P[42] of –0.56 corresponded to the polarity of the hydroxyl group (O-H) and the secondary amine that allows the formation of hydrogen bonds with water. The dipole moment of the diuron (see Figure 2b) was attributed to the electronegativity of the oxygen of the carbonyl group and chlorine atoms, while the log P indicated that the diuron[43] interacts with water due to the presence of a polar molecule such as secondary amine, which forms hydrogen bonds with water due to its physical properties. Finally, the log P of atrazine[44] (see Figure 2c) indicated a hydrophobic character due to the presence of tertiary amines (triazine group).

Table 1. Thermodynamic and QSAR properties of pesticides

Thermodynamic properties			
Properties	Glyphosate	Diuron	Atrazine
Gibbs free energy / (kcal mol^{-1})	–51527.30	–57011.70	–52869.40
Enthalpy / (kcal mol^{-1})	–286.80	–29.27	4.79
Bond energy / (kcal mol^{-1})	–1702.65	–2431.84	–2685.74
Dipole moment / Debyes (D)	0	4.54	3.43
QSAR properties			
Mass / amu	169.07	233.10	215.69
Volume / $Å^3$	473.17	648.16	683.76
log P	-0.56	-0.52	3.29
Surface area / $Å^2$	324.13	411.13	437.60

The determination of melting point and solubility, Equation 1, allows to determine the radius (r) of a molecule where V is expressed in $Å^3$,[31] which is used to obtain the melting point, the theoretical solubility, and the surface that an adsorbent has available (SWCNT) to interact with the pesticide, i.e., the ASA on the adsorbent.

$$r = \left(\frac{3V}{4\pi}\right)^{\frac{1}{3}} \quad (1)$$

The melting point (MP) in °C of each molecule was determined with Equation 2, where m is expressed in amu units and nC represents the number of carbons in the structure.[32] On the other hand, with Equation 3 the solubility in mol L^{-1} was determined.[45]

$$MP = 117 + 0.142m - 0.79nC \quad (2)$$

$$\log 10sw = -0.01PF - \log P + 1.05 \quad (3)$$

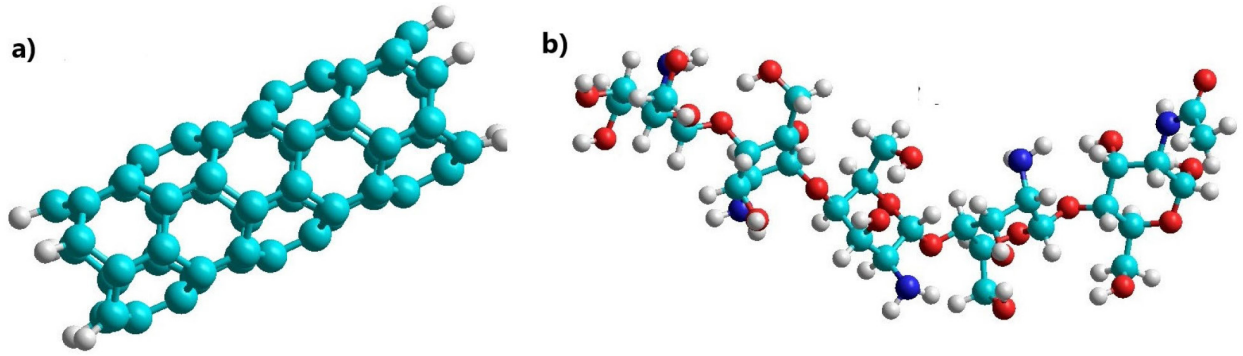

Figure 1. *Molecular structure of (a) SWCNT and, (b) chitosan, where; oxygen: red color, carbon: cyan color, nitrogen: blue color and chlorine: black color, respectively*

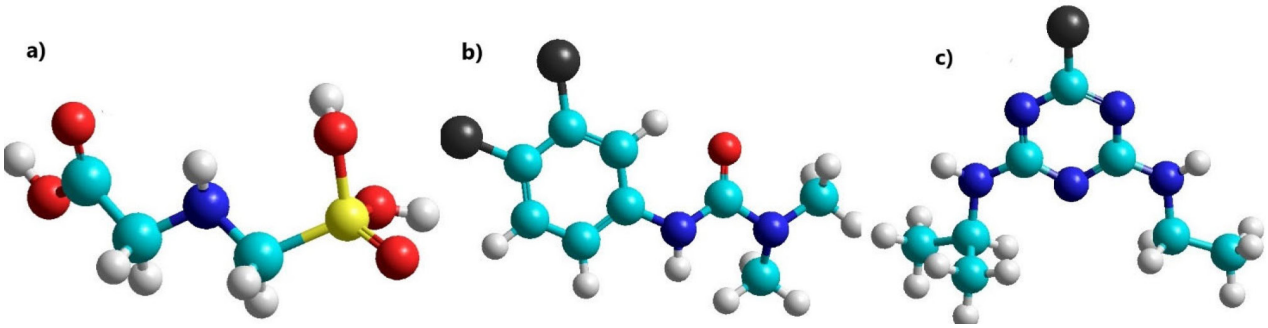

Figure 2. *Molecular structure of (a) glyphosate, (b) diuron and, (c) atrazine, where; oxygen: red color, carbon: cyan color, phosphorus: yellow color, nitrogen: blue color and chlorine: black color, respectively*

RESULTS AND DISCUSSION

Some authors[46-49] have determined that the mixture of sulfuric and nitric acid for the oxidation of SWCNT generates the formation of nitronium ions (NO^{2+}), which is responsible for adding oxygen to the SWCNT structure, producing the formation of carbonyl groups (C=O), phenol (OH) and carboxylic acid (COOH). Figure 3 shows the electron distribution map (ESP) of the SWCNT with the NO^{2+} ion (SWCNTox), which was obtained by the PM3 semi-empirical method, where the sites susceptible to electrophilic attacks were in the structure of the SWCNT (blue color) and the nucleophiles in the oxygens of the NO^{2+} ion (red color) producing that, the π bonds of C=C fragmented into free electrons and formed C=O, OH and COOH groups. The number of sites available for the formation of these groups was related to the number of nucleophilic attacks (four sites), however, as there is a delocalization of the π electrons and free electrons, five available sites were obtained.

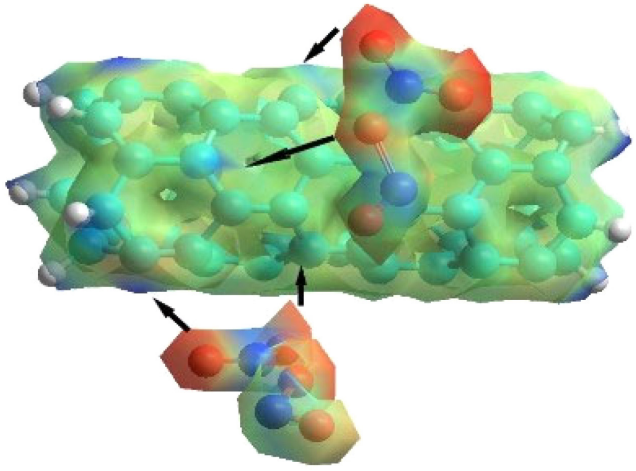

Figure 3. *MESP of the SWCNT functionalized at 298.15 K*

In addition, oxidation by H_2SO_4/HNO_3 with oxidation times of less than 18 h, firstly, the C=O bond is obtained in higher concentration, then OH and COOH. In this case, three C=O groups, one OH and one COOH were placed, corresponding to the number of sites available for electrophilic attacks.[46-49] The log P (6.95), mass (840.76 amu), AS / V (629.45 $Å^2$ / 523.36 $Å^3$, respectively) and r (5.3165 Å) were obtained according to Figure 4.

SWCNTox/chitosan crosslinking

The SWNTox/chitosan (SWCNTox/Q) crosslinking was determined by PM3 semi-empirical method through the C=O and OH bonds of chitosan with a bond groups in the oxidation process, but

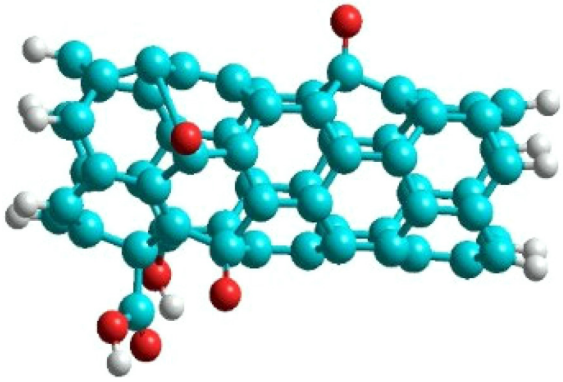

Figure 4. *Molecular structure of SWCNTox at 298.15 K*

if the OH groups increase then the interactions with chitosan would be stronger. Yan *et al.*[50] determined through molecular dynamics that the bond distance of C=O (SWCNTox) and OH (chitosan) was 5 Å respectively. So, using the PM3 semi-empirical method and Monte Carlo simulation, the values are in the range reported for hydrogen bonds.[51,52]

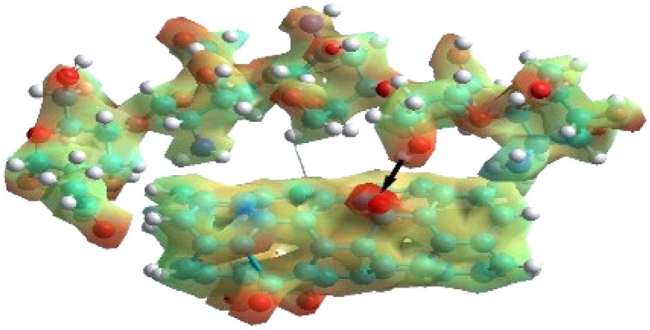

Figure 5. *MESP of the SWCNTox/Q crosslinking at 298.15 K*

Table 2 shows the energetic properties of the formation of the SWCNTox and the SWCNTox/Q crosslinking were of a non-spontaneous nature, which coincides with the synthesis method where high temperatures are required.[53,54] On the other hand, the enthalpy indicated that SWCNTox and SWCNTox/Q are endothermic.

The dipole moment increased in SWCNTox/Q due to the electronic density of the groups C=O, OH, COOH, P=O, NH_2, NH and C–O–C, which have a high charge due to the pair of free electrons mainly in oxygen and nitrogen, therefore, the molecules are polar.

Monte Carlo simulation calculated the QSAR properties (see Table 3), which show that diuron and glyphosate presented affinity for water due to the OH and NH groups. Atrazine was hydrophobic due to the C=N and CH_3 bond of atrazine, respectively. SWCNTox/Q is hydrophilic attributed to the interaction of OH bonds and C=C sp^2

Table 2. Energetic properties of molecules at 298.15 K

Properties	SWCNTox	SWCNTox/Q
Gibbs free energy / (kcal mol^{-1})	866.98	23.31
Enthalpy / (kcal mol^{-1})	924.61	149.96
Bond energy / (kcal mol^{-1})	0.193	0.424
Dipole moment / Debyes (D)	7.22	11.59

SWCNTox: single-walled carbon nanotube functionalized; SWCNTox/Q: single-walled carbon nanotube functionalized crosslinked with chitosan.

hybridization in the SWCNT structure. Using Equation 1, it was observed in Table 4 that SWCNTox/Q has a greater contact area with atrazine compared to diuron and glyphosate, respectively. In addition, the temperature that showed the largest contact surface was 291.15 K, because atrazine has a larger radius compared to diuron and glyphosate.

However, the degree of hydrophobicity is not considered, so it was necessary to calculate the fraction of the SWCNTox/Q surface that was used in the adsorption process, and it was calculated by dividing the AS of the adsorbent with respect to the ASA of each pesticide at the different temperatures (AS/ASApesticide). The increase in temperature determined that diuron and atrazine increased with the temperature (see Table 5). SWCNTox/Q has a carbon number (nC) of 93 and a melting point of 285.87 °C and using Equations 2 and 3 the Swcalc of 1.554 mol L^{-1} was determined, because SWCNTox/Q tends to solubilize in greater proportion than pesticides, which was attributed to the protonation or deprotonation of the NH, C=O and OH groups.[55]

Monocomponent adsorption Monte Carlo simulation indicated that the adsorption processes of the pesticides in the SWCNTox/Q were thermodynamically stable due to the G (Gibbs free energy), which is related to the positive S (entropy) where a better affinity between the adsorbate-adsorbent was observed (see Table 6).[56,57] On the other hand, the H (enthalpy) indicated that the adsorption of glyphosate was an exothermic process and for diuron and atrazine endothermic, that is, the adsorption capacity of glyphosate decreases, while diuron and atrazine increased with temperature,[58] which coincides with the results obtained from the fraction of the adsorbent used (see Table 4).

However, there is a discrepancy with the G and S of the SWCNTox/Q-glyphosate, because the value of G at 291.15 K should be less than that of 298.15 K and for S it should be higher respectively, which can be attributed to that the influence of pH has not been taken, that is, glyphosate has groups that tend to protonation-deprotonation

Table 3. QSAR properties by Monte Carlo simulation

Molecule	Temperature / K	log P	Volume / Å^3	Radius / Å	Surface area / Å^2	Mass / amu
SWCNTox/Q	291.15	–21.00	1338.87	6.8373	1354.82	1706.60
	298.15		1344.05	6.8461	1352.98	
Glyphosate	291.15	–0.56	123.57	3.0890	170.60	169.07
	298.15		123.73	3.0912	170.91	
Diuron	291.15	–0.52	190.58	3.5699	228.27	233.10
	298.15		190.19	3.5675	228.51	
Atrazine	291.15	3.29	194.69	3.5954	244.89	215.69
	298.15		195.64	3.6013	246.00	

log P: octanol-water partition coefficient.

Table 4. Accesible surface area of the adsorbent for each pesticide at different temperature

Molecule	Temperature / K	ASA^{Glyphosate} / Å^2	ASA^{Diuron} / Å^2	ASA^{Atrazine} / Å^2
SWCNTox/Q	291.15	1833.04	1990.56	1998.34
	298.15	1831.87	1981.60	1991.05

ASA: accessible surface area; SWCNTox/Q: single-walled carbon nanotube functionalized crosslinked with chitosan.

Table 5. Fraction of ASA used in the adsorption for each pesticide

Molecule	Temperature / K	ASA^{Glyphosate} / Å^2	ASA^{Diuron} / Å^2	ASA^{Atrazine} / Å^2
SWCNTox/Q	291.15	0.7391	0.6806	0.6780
	298.15	0.7386	0.6828	0.6795

ASA: accessible surface area; SWCNTox/Q: single-walled carbon nanotube functionalized crosslinked with chitosan.

Table 6. Thermodynamic properties of SWCNTox/Q-pesticide adsorption

System	Temperature / K	G / (kcal mol^{-1})	H / (kcal mol^{-1})	S / (kcal mol^{-1})	M / Debyes
SWCNTox/Q-glyphosate	291.15	–253.89	–121.96	0.453	12.03
	298.15	–283.97	–145.99	0.462	12.74
SWCNTox/Q-diuron	291.15	–4.07	125.17	0.443	15.77
	298.15	–15.00	126.78	0.475	16.27
SWCNTox/Q-atrazine	291.15	–2.43	128.51	0.449	8.55
	298.15	–10.38	124.10	0.451	9.18

SWCNTox/Q: single-walled carbon nanotube functionalized crosslinked with chitosan; G: Gibbs free energy; H: enthalpy; S: entropy; M: dipole moment.

(three p*K*a ranges),[59,60] which influences the thermodynamic and QSAR properties. Finally, the dipole moment showed a linear relationship with the increase in temperature and this phenomenon is mainly attributed to the change in the bond distances and the quantum leaps of the electrons caused by the increase in the temperature.

On the other hand, the QSAR properties (see Table 7) indicated that all systems were soluble in water after adsorption at 291.15 and 298.15 K respectively. Atrazine, which is a hydrophobic molecule, when in contact with SWCNTox/Q, its degree of hydrophobicity is lower compared to glyphosate and diuron, respectively. This phenomenon was attributed to the lower capacity of atrazine to form hydrogen bonds due to the electronegativity of amines. While glyphosate and diuron are composed of elements with higher electronegativity, such as oxygen. Therefore, the QSAR properties in the adsorption are a fundamental parameter to be able to recover the adsorbent or the adsorbate by physicochemical methods which are influenced by solubility.[61] The adsorption at different temperatures (291.15 and 298.15 K) showed that the V, AS, and the radius increased because the positions of the electrons changed with respect to the nucleus and consequently a change in their radius, VM and AM.

The adsorption of the pesticides in the SWCNTox/Q was carried out by hydrogen bonds with moderate (1.5-2.2 Å) and weak (2.0-3.2 Å) strength,[51,52] as observed in Table 8. According to these values, the adsorption process was by physisorption or intermolecular forces due to the high electronegativity of C–O, OH, NH_2, NH and C=O. Considering that hydrophilic molecules interact better in an aqueous system, glyphosate and diuron do so more strongly compared to atrazine.

Thus, the adsorption of glyphosate was in the C–O–C of chitosan (see Figure 6), while the diuron formed hydrogen bonds between the C=O of diuron and the OH of chitosan, because the electronic density of the carbonyl group is greater with respect to the secondary and tertiary amines of diuron (see Figure 7). Finally, the adsorption of atrazine in the SWCNTox/Q system was between the hydrogen of the primary amine and the nitrogen of the secondary amine respectively (see Figure 8).

Table 7. QSAR properties of SWCNTox/Q-pesticide adsorption by Monte Carlo simulation

System	Temperature / K	Mass / amu	log P	Volume / Å^3	Surface area / Å^2
SWCNTox/Q-glyphosate	291.15	1875.68	–24.08	1462.65	1496.29
	298.15			1465.70	1501.51
SWCNTox/Q-diuron	291.15	1939.70	–23.33	1525.60	1551.20
	298.15			1527.70	1559.42
SWCNTox/Q-atrazine	291.15	1922.29	–22.36	1532.33	1575.35
	298.15			1530.21	1574.30

QSAR: quantitative structure activity relationship; SWCNTox/Q: single-walled carbon nanotube functionalized crosslinked with chitosan; log P: octanol-water partition coefficient.

Table 8. Bond length of each system

System	Temperature / K	Bond	Bond length	Intensity
SWCNTox/Q-glyphosate	291.15	C-O-C → COOH	1.907	moderate
	298.15		1.848	
SWCNTox/Q-diuron	291.15	C-OH → C=O	1.911	moderate
	298.15		1.889	
SWCNTox/Q-atrazine	291.15	NH_2 → NH	2.691	weak
	298.15		2.807	

SWCNTox/Q: single-walled carbon nanotube functionalized crosslinked with chitosan.

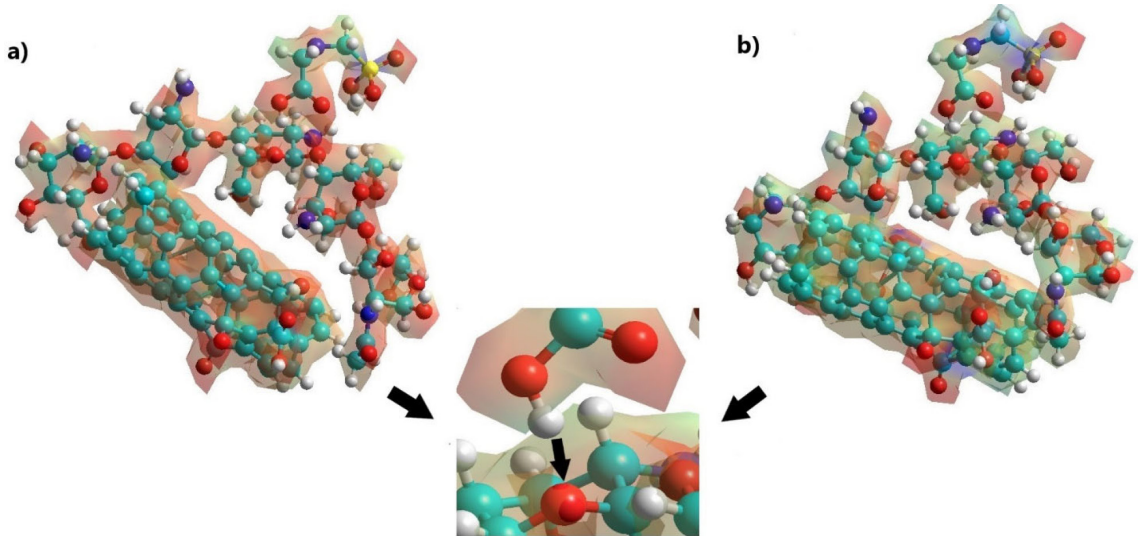

Figure 6. *MESP of the SWCNTox/Q-glyphosate adsorption: (a) 291.15 and (b) 298.15 K*

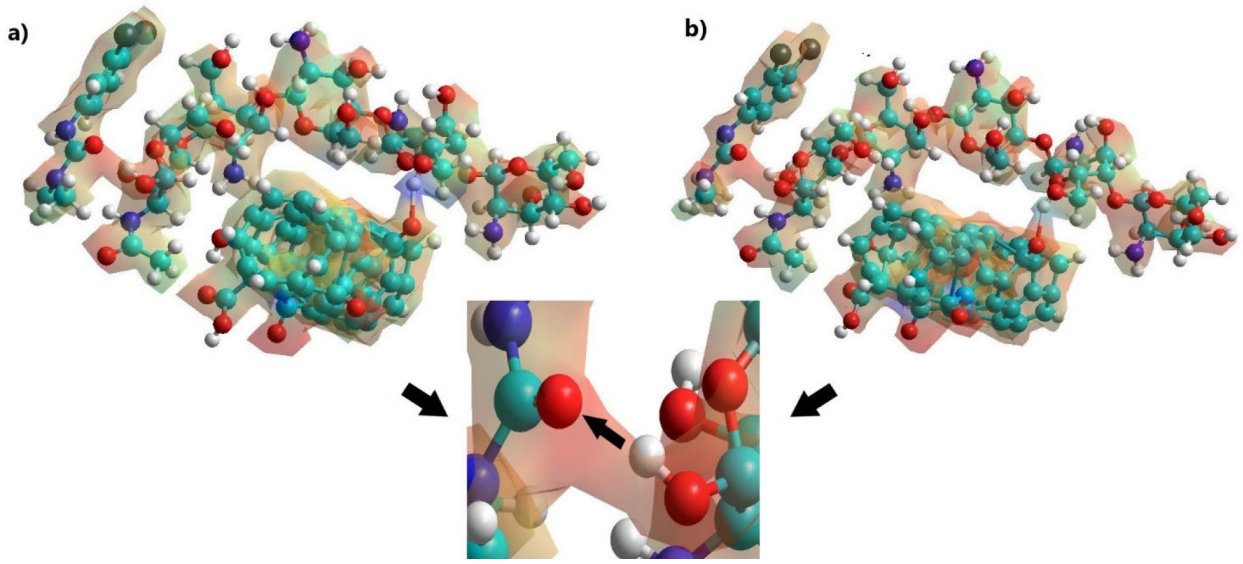

Figure 7. *MESP of the SWCNTox/Q-diuron adsorption: (a) 291.15 and (b) 298.15 K*

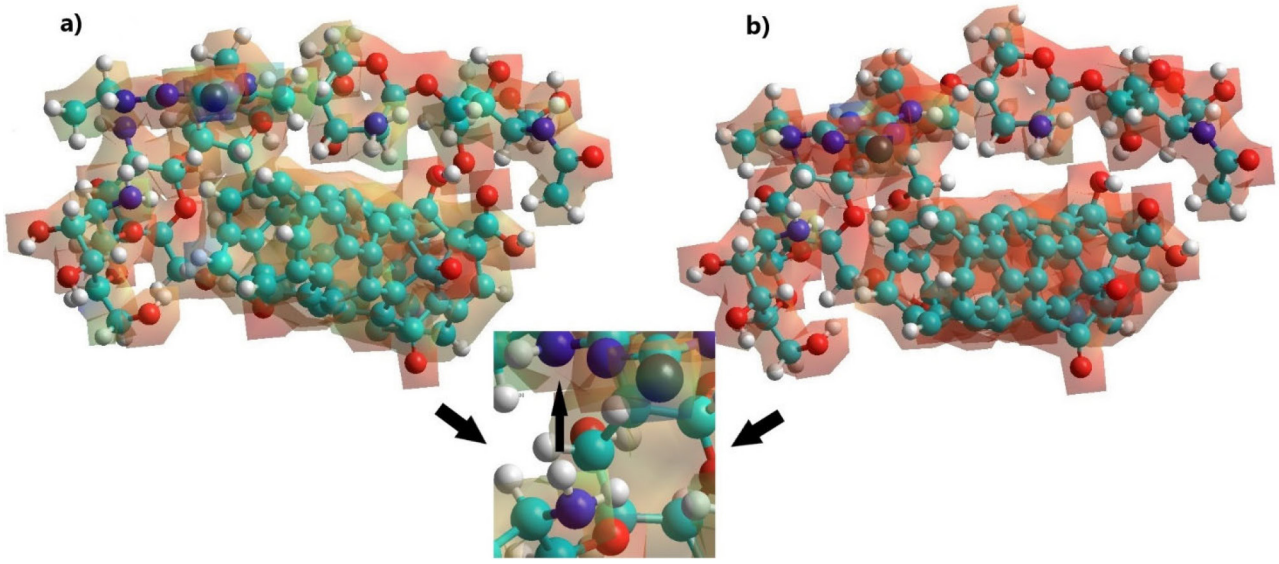

Figure 8. *MESP of the SWCNTox/Q-atrazine adsorption: (a) 291.15 and (b) 298.15 K*

CONCLUSIONS

The carbonyl (C=O), phenol and carboxylic groups allowed the oxidation of the SWCNT on the surface due to the formation of several active sites attributed to a delocalization of the π electrons and free electrons. The formation of hydrogen bonds allowed the crosslinking of SWCNTox and chitosan through the C=O and OH groups, respectively. The log P indicated the solubility of the SWCNTox/chitosan in polar solvents. Pesticide adsorption on SWCNTox/chitosan was spontaneous and exothermic for glyphosate while diuron and atrazine were endothermic. The Monte Carlo modeling indicated that the adsorption at different temperatures (291.15 and 298.15 K) was spontaneous, indicating a physisorption process due to the electronegativity of the C–O, OH, NH_2, NH and C=O bonds, respectively, it was also observed that, volume (V), surface area (AS), and radius increased.

SUPPLEMENTARY MATERIAL

Complementary material for this work is available at http://quimicanova.sbq.org.br/, as a PDF file, with free access.

ACKNOWLEDGMENTS

Alfredo de Jesús González thanks CONAHCYT for the scholarship granted for the Doctorate in Engineering Sciences.

REFERENCES

1. Dai, L.; Lu, Q.; Zhou, H.; Shen, F.; Liu, Z.; Zhu, W.; Huang, H.; *J. Hazard. Mater.* **2021**, *420*, 126547. [Crossref]
2. Bao, Z. Z.; Chen, Z. F.; Lu, S. Q.; Wang, G.; Qi, Z.; Cai, Z.; *Sci. Total Environ.* **2021**, *790*, 148077. [Crossref]
3. Malla, M. A.; Gupta, S.; Dubey, A.; Kumar, A.; Yadav, S. In *Contamination of Water*; Ahamad, A.; Siddiqui, S. I.; Singh, P., eds.; Academic Press: Cambridge, 2021, ch. 7.
4. Martins-Gomes, C.; Silva, T. L.; Andreani, T.; Silva, A. M.; *J. Xenobiot.* **2022**, *12*, 21. [Crossref]
5. Kalogiannidis, S.; Kalfas, D.; Chatzitheodoridis, F.; Papaevangelou, O.; *Land* **2022**, *11*, 1680. [Crossref]
6. Bexfield, L. M.; Belitz, K.; Lindsey, B. D.; Toccalino, P. L.; Nowell, L. H.; *Environ. Sci. Technol.* **2021**, *55*, 362. [Crossref]
7. Syafrudin, M.; Kristanti, R. A.; Yuniarto, A.; Hadibarata, T.; Rhee, J.;

Al-onazi, W. A.; Algarni, T. S.; Almarri, A. H.; Al-Mohaimeed, A. M.; *Int. J. Environ. Res. Public Health* **2021**, *18*, 468. [Crossref]
8. Mukhopadhyay, R.; Sarkar, B.; Jat, H. S.; Sharma, P. C.; Bolan, N. S.; *J. Environ. Manage.* **2021**, *280*, 111736. [Crossref]
9. Zaluski, A. B.; Wiprich, M. T.; de Almeida, L. F.; de Azevedo, A. P.; Bonan, C. D.; Vianna, M. R. M.; *Front. Pharmacol.* **2022**, *4*, 841826. [Crossref]
10. Valavanidis, A.; *Scientific Reviews* **2018**, *1*, 1. [Link] accessed in May 2024
11. Cox, C.; *Journal of Pesticide Reform* **1993**, *13*, 4. [Link] accessed in May 2024
12. Ghazi, R. M.; Yusoff, N. R.; Halim, N. S. A.; Wahab, I. R. A.; Latif, N. A.; Hasmoni, S. H.; Zaini, M. A. A.; Zakaria, Z. A.; *Bioengineered* **2023**, *14*, 1. [Crossref]
13. Diel, J. C.; Martinello, K. B.; da Silveira, C. L.; Pereira, H. A.; Franco, D. S. P.; Silva, L. F. O.; Dotto, G. L.; *Chem. Eng. J.* **2022**, *431*, 134095. [Crossref]
14. Maheswaran, R.; Shanmugavel, B. P.; *J. Electron. Mater.* **2022**, *51*, 2786. [Crossref]
15. Sebastian, F. L.; Becker, F.; Yomogida, Y.; Hosokawa, Y.; Settele, S.; Lindenthal, S.; Yanagi, K.; Zaumseil, J.; *ACS Nano* **2023**, *17*, 21771. [Crossref]
16. Bosco, C. D.; de Cesaris, M. G.; Felli, N.; Lucci, E.; Fanali, S.; Gentili, A.; *Mikrochim. Acta* **2023**, *190*, 175. [Crossref]
17. Hoang, A. T.; Nižetić, S.; Cheng, C. K.; Luque, R.; Thomas, S.; Banh, T. L.; Pham, V. V.; Nguyen, X. P.; *Chemosphere* **2022**, *287*, 131959. [Crossref]
18. Peng, J.; Zhou, P.; Zhou, H.; Huang, B.; Sun, M.; He, C. S.; Zhang, H.; Ao, Z.; Liu, W.; Lai, B.; *Environ. Sci. Technol.* **2023**, *57*, 10804. [Crossref]
19. Horibe, A.; Murayama, T.; Kawai, T.; Nonoguchi, Y.; *RSC Applied Interfaces* **2024**, *1*, 80. [Crossref]
20. Văduva, M.; Burlănescu, T.; Baibarac, M.; *Polymers* **2024**, *16*, 53. [Crossref]
21. Xavier, J. R.; Pandian, V. S.; *Polym. Eng. Sci.* **2023**, *63*, 9. [Crossref]
22. Almarri, A. H.; *Int. J. Environ. Anal. Chem.* **2023**, *103*, 3212. [Crossref]
23. Magid, M.; Al-Karam, L. Q.; *J. Phys.: Conf. Ser.* **2021**, *2114*, 1. [Crossref]
24. Gulati, S.; Lingam, B. H. N.; Kumar, S.; Goyal, K.; Arora, A.; Varma, R. S.; *Chemosphere* **2022**, *299*, 134468. [Crossref]
25. Spaolonzi, M. P.; Duarte, E. D. V.; Oliveira, M. G.; Costa, H. P. S.; Ribeiro, M. C. B.; Silva, T. L.; Silva, M. G. C.; Vieira, M. G. A.; *J. Cleaner Prod.* **2022**, *373*, 133961. [Crossref]
26. Sajid, M.; Asif, M.; Baig, N.; Kabeer, M.; Ihsanullah, I.; Mohammad, A. W.; *Journal of Water Process Engineering* **2022**, *47*, 102815. [Crossref]
27. Shadpour, M.; Elham, A.; Mustansar, H. C.; *New J. Chem.* **2021**, *45*, 3756. [Crossref]
28. Hsieh, C. J.; Giannakoulias, S.; Petersson, E. J.; Mach, R. H.; *Pharmaceuticals* **2023**, *16*, 317. [Crossref]
29. Choudhuri, S.; Yendluri, M.; Poddar, S.; Li, A.; Mallick, K.; Mallik, S.; Ghosh, B.; *Kinases Phosphatases* **2023**, *1*, 117. [Crossref]
30. Townsend, P. A.; *ACS Omega* **2024**, *9*, 5142. [Crossref]
31. Bastikar, V.; Bastikar, A.; Gupta, P. In *Computational Approaches for Novel Therapeutic and Diagnostic Designing to Mitigate SARS-CoV-2 Infection - Revolutionary Strategies to Combat Pandemics*; Parihar, A.; Kumar, A.; Gohel, H.; Kan, R.; Kaushik, A. K., eds.; Academic Press: Cambridge, 2022, p. 191. [Crossref]
32. Soares, T. A.; Alves, A. N.; Mazzolari, A.; Ruggiu, F.; Wei, G.; Merz, K.; *J. Chem. Inf. Model.* **2022**, *62*, 5317. [Crossref]
33. Savojardo, C.; Manfredi, M.; Martelli, P. L.; Casadio, R.; *Front. Mol. Biosci.* **2021**, *7*, 1. [Crossref]
34. Bhatt, P.; Joshi, T.; Bhatt, K.; Zhang, W.; Huang, Y.; Chen, S.; *J. Hazard. Mater*. **2020**, *409*, 124927. [Crossref]
35. Galicia-Andrés, E.; Tunega, D.; Gerzabek, M. H.; Oostenbrink, C.; *Eur. J. Soil Sci.* **2021**, *72*, 1231. [Crossref]
36. Tlemsania, S.; Taleba, Z.; Pirault-Royb, L.; Taleb, S.; *Int. J. Environ. Anal. Chem.* **2022**, 1. [Link] accessed in May 2024
37. Sun, H.; Jiang, Y. F.; Shi, L. P.; Mu, Z. F.; Zhan, H. Y.; *Huan Jing Ke Xue* **2016**, *37*, 4857. [Crossref]
38. Pitt Quantum Repository, https://pqr.pitt.edu/mol/xmtqqyykahvgbj-uhfffaoysa-n, accessed in May 2024.
39. Pitt Quantum Repository, https://pqr.pitt.edu/mol/dfwfiqkmsfgdcq-uhfffaoysa-n, accessed in May 2024.
40. Yu, X.; Zhou, C. R.; Han, X. W.; Li, G. P.; *J. Therm. Anal. Calorim.* **2013**, *111*, 943. [Crossref]
41. Haynes, W. M.; *CRC Handbook of Chemistry and Physics*, 95th ed.; CRC Press: Boca Raton, Florida, 2014.
42. Kanissery, R.; Gairhe, B.; Kadyampakeni, D.; Batuman, O.; Alferez, F.; *Plants* **2019**, *8*, 499. [Crossref]
43. Gianni, E.; Moreno-Rodríguez, D.; Jankovič, Ľ.; Scholtzová, E.; Pospíšil, M.; *J. Environ. Chem. Eng.* **2022**, *10*, 108785. [Crossref]
44. Cheremisinoff, N. P.; Rosenfeld, P. E.; *Handbook of Pollution Prevention and Cleaner Production: Best Practices in the Agrochemical Industry*,1st ed.; William Andrew: Oxford, 2011.
45. Mohr, T. K. G.; Hatton, J. W. In *Environmental Investigation and Remediation*; Mohr, T. K. G.; DiGuiseppi, W. H.; Anderson, J. K.; Hatton, J. W., eds.; CRC Press: Boca Raton, USA, 2020, ch. 3.
46. Guo, Q.; Zhao, Y.; Lei, Y.; Li, G.; He, Y.; Zhang, G.; Zhang, Y.; Li, K.; *ACS Omega* **2023**, *8*, 25938. [Crossref]
47. Wojtera, K.; Walczak, M.; Pietrzak, L.; Fraczyk, J.; Szymanski, L.; Sobczyk-Guzenda, A.; *Nanotechnol. Rev.* **2020**, *9*, 1237. [Crossref]
48. Chio, L.; Pinals, R. L.; Murali, A.; Goh, N.; Landry, M. P.; *Adv. Funct. Mater*. **2020**, *30*, 1910556. [Crossref]
49. Gu, M.; Zhao, Z.; Jiaxuan, L.; Lui, G.; Zhang, B.; El-Khouly, M. E.; Chen, Y.; *Eur. Polym. J.* **2021**, *142*, 110153. [Crossref]
50. Yan, T.; Wu, Y.; Yi, W.; Pan, Z.; *Sens. Actuators, A* **2021**, *327*, 112755. [Crossref]
51. Kohmuean, P.; Inthomya, W.; Wongkoblap, A.; Tangsathitkulchai, C.; *Molecules* **2021**, *26*, 2413. [Crossref]
52. Grabowski, S. J.; *Coord. Chem. Rev.* **2020**, *407*, 213171. [Crossref]
53. Wu, Q.; Qiu, L.; Zhang, L.; Liu, H.; Ma, R.; Xie, P.; Liu, R.; Hou, P.; Ding, F.; Liu, C.; He, M.; *Chem. Eng. J.* **2022**, *431*, 133487. [Crossref]
54. Yang, F.; Wang, M.; Zhang, D.; Yang, J.; Zheng, M.; Li, Y.; *Chem. Rev.* **2020**, *120*, 2693. [Crossref]
55. Cooper, M.; Klymkowsky, M.; *OCLUE: Organic Chemistry, Life, the Universe & Everything*, 1st ed.; Michigan State University Libraries: Michigan, 2020.
56. Kosheleva, R. I.; Karapantsios, T. D.; Kostoglou, M.; Mitropoulos, A.; *J. Non-Equilib. Thermodyn.* **2023**, *48*, 403. [Crossref]
57. Oche, D.; Louis, H.; Bassey, V. M.; Okon, G. A.; Edet, H. O.; Jumbo, J. T.; Adeyinka, A. S.; *Results Chem.* **2023**, *5*, 100980. [Crossref]
58. Al-Ghouti, M. A.; Al-Absi, R. S.; *Sci. Rep.* **2020**, *10*, 15928. [Crossref]
59. Kovács, N.; Maász, G.; Galambos, I.; Gerencsér-Berta, R.; Mihály, J.; Tombácz, E.; *J. Mol. Liq.* **2024**, *393*, 123674. [Crossref]
60. Agostini, L. P.; Dettogni, R. S.; dos Reis, R. S.; Stur, E.; dos Santos, E. V. W.; Ventorim, D. P.; Garcia, F. M.; Cardoso, R. C.; Graceli, J. B.; Louro, I. D.; *Sci. Total Environ.* **2020**, *705*, 135808. [Crossref]
61. Webb, D. T.; Nagorzanski, M. R.; Cwiertny, D. M.; LeFevre, G. H.; *ACS ES&T Water* **2022**, *2*, 247. [Crossref]